Temperature-Dependent, Irreversible Formation of Amyloid Fibrils by a Soluble Human Ataxin-3 Carrying a Moderately Expanded Polyglutamine Stretch (Q36)†

Erlet Shehi,‡,§ Paola Fusi,‡,§ Francesco Secundo,|| Sabrina Pozzuolo,‡ Aurelio Bairati,⊥ and Paolo Tortora*,‡

Dipartimento di Biotecnologie e Bioscienze, Università di Milano−Bicocca, Piazza della Scienza 2, I-20126 Milano, Italy, Istituto di Chimica del Riconoscimento Molecolare, C. N. R., Via Mario Bianco 9, I-20131, Milano, Italy, and Dipartimento di Scienze Biomolecolari e Biotecnologie, Università di Milano, Via Celoria 26, I-20133 Milano, Italy

Received July 19, 2003; Revised Manuscript Received October 8, 2003

ABSTRACT: The protein ataxin-3 is responsible for Machado−Joseph disease/spinocerebellar ataxia type 3, a neurodegenerative disorder caused by the presence of an expanded polyglutamine tract. A previous investigation [Bevivino, A. E., and Loll, P. J. (2001) *Proc. Natl. Acad. Sci. U.S.A. 98,* 11955−11960] showed that a nonexpanded ataxin-3 (Q27) was fully soluble, whereas an expanded form (Q78) gave rise to amyloid fibrils. Here, we report investigations on three forms of ataxin-3 (i.e., human nonexpanded (Q26), moderately expanded (Q36) ataxins-3, and the murine protein (Q6)). Far-UV circular dichroism spectra at room temperature were substantially similar, with a relatively high helical content. On heating to 96 °C, human Q26 and murine proteins did not display large structural changes, nor did they undergo any precipitation, which highlights their amazing heat-resistance. In contrast, human Q36 ataxin-3 underwent a progressive increase in the β-sheet and a concomitant decrease in helical content when the temperature was shifted from 37 to 80 °C, followed by the irreversible formation of aggregates above 80 °C. They were shown to consist of amyloid fibrils, as supported by both electron microscopy images and the typical spectral shift displayed by Congo red when it was added to the protein at growing temperatures. We also found that protein precipitation could be prevented by mixing the dye with Q36 ataxin-3 prior to heating, which also confirms that the precipitates do represent authentic amyloid fibrils. In contrast, other compounds structurally related to Congo red did not exert significant effects. Our observations suggest that the temperature of the observed transition is inversely related to the length of the expansion. Finally, we suggest that antiamyloidogenic compounds might be selected on the basis of their ability to block or retard human Q36 ataxin-3 precipitation on heat-treatment.

Polyglutamine[1] (polyQ) diseases are late-onset inherited neurodegenerative disorders caused by the presence of glutamine repeats exceeding a critical size, typically 35−40 consecutive residues, in a number of proteins (*1*−*3*). No size or sequence similarity is apparent among the proteins responsible for these neurodegenerative disorders. However, the striking similarities in genetic, clinical, neuropathological, and molecular features among polyQ diseases suggest that they share the fundamental mechanisms of pathogenesis, based on a toxic gain of function at the protein level (*1*, *4*). Thus, glutamine expansions beyond the critical size are thought to both induce conformational modifications in the host protein and promote protein aggregation by acting as polar zippers (*5*, *6*). This results in the formation of insoluble aggregates, mostly nuclear (*1*), which also recruit additional proteins, among others, and transcription factors or other regulatory nuclear proteins (*7*).

Despite the remarkable similarities among polyQ diseases, significant differences at the clinical and cellular level are also evident. In particular, selective neuronal loss strikes different brain regions in different diseases (*2*, *8*). This points to mechanisms of pathogenesis that involve varying expression levels in different neurons and/or different molecular partners recruited by the polyglutaminated proteins in different intracellular milieus.

Although the causal relationships among the individual events that eventually lead to neurodegeneration are still poorly understood, it seems likely that the appearance of aggregates represents the primary event triggering the downstream pathological manifestations (*9*−*11*), or at least, that the aggregation process is linked to pathogenesis (*8*). In keeping with this idea, it was observed that inhibition of PolyQ oligomerization by CR in a transgenic mouse model of Huntington disease preserved cellular functions and exerted protective effects on survival, weight loss, and motor function (*12*). Thus, considerable efforts are being directed toward the development of screening assays aimed at selecting polyglutamine aggregation inhibitors as drugs capable to treat polyQ diseases (*13*).

† Work supported by grants from Telethon, Italy (Project 1021) and from the Hereditary Disease Foundation, U.S.A.

* Corresponding author. Phone: (+39) 02 6448 3401. Fax: (+39) 02 6448 3565. E-mail: paolo.tortora@unimib.it.

‡ Università di Milano−Bicocca.

§ Authors who equally contributed to the work.

|| Istituto di Chimica del Riconoscimento Molecolare.

⊥ Università di Milano.

[1] Abbreviations: polyQ, polyglutamine; IPTG, isopropyl β-D-thiogalactopyranoside; DTT, dithiothreitol; GST, glutathione *S*-transferase; SDS−PAGE, sodium dodecyl sulfate−polyacrylamide gel electrophoresis; PVDF, polyvinylidene fluoride; CD, circular dichroism; CR Congo red.

10.1021/bi0352825 CCC: $25.00
Published on Web 11/19/2003

Relevant to therapeutic strategies devised to prevent or reverse aggregation is the understanding of the structural differences between nonexpanded and expanded polyQ stretches. So far, most available structural data were obtained either from investigations carried out on artificial constructs (*6*, *14*−*16*) or from a computer-generated model (*5*).

Only recently, the structure of an authentic polyglutaminated protein (i.e., human ataxin-3), both nonexpanded (Q27) and expanded (Q78), was investigated using CD (*17*). This is a widely expressed protein, which causes Machado−Joseph disease/spinocerebellar ataxia type 3 via selective damage, mainly of cerebellar dentate neurons, basal ganglia, the brain stem, and the spinal cord (*2*). Its physiological localization is cytoplasmic, but pathological variants give rise to nuclear inclusions. Ataxin-3 has no obvious homology to any other known protein, nor is its physiological role well-understood, although recent findings suggest that it is a histone-binding protein with two independent transcriptional corepressor activities (*18*). The aforementioned authors (*17*) found that human Q27 ataxin-3 is fully soluble and has a relatively high helical content, whereas the Q78 variant is only soluble when expressed with the maltose-binding protein as a fusion partner. They also observed that, under these conditions, the Q78 protein had a much lower helical content than the Q27 form and that, upon proteolytic removal of the fusion partner, it became insoluble, thus giving rise to fibrils with a high β-structure content.

To gain further insight into the role of polyQ tracts on protein stability and solubility, we investigated three different forms of ataxin-3 (i.e., murine (Q6), human nonexpanded (Q26), and human moderately expanded (Q36)). Our interest in a moderately expanded form is justified by the fact that proteins carrying longer expansions can be hardly kept in solution, which prevents thorough structural characterization. Furthermore, investigations on proteins with relatively short expansions may help better understand the role of the protein context, which actually can significantly affect polyQ solubility (*15*). Our findings show that, whereas Q6 and Q26 ataxins-3 are amazingly thermostable, the Q36 variant gives rise to amyloid fibrils on increasing temperature above 40 °C.

EXPERIMENTAL PROCEDURES

Gene Cloning. A cDNA encoding murine ataxin-3 was identified searching the EST database (dbEST) for entries showing homology with human ataxin-3. The best alignment (91% identity) was obtained with NCI CGAP Kid14 Mus musculus cDNA (dbEST ID: 7279528). The corresponding IMAGE clone (IMAGE:4234485) was obtained from the RZPD Deutsches Resourcenzentrum für Genomforschung GmbH. Murine ataxin-3 cDNA was isolated by PCR using gene-specific oligonucleotide primers and subsequently cloned into plasmid pGEX-6P-1 (Amersham Biosciences UK Ltd., Little Chalfont, England). This plasmid allows cloning of foreign genes under an IPTG-inducible tac promoter. Recombinant proteins can be expressed as GST fusion proteins and retrieved by means of a PreScission Protease (Amersham Biosciences UK Ltd., Little Chalfont, England) cleavage site located between the two coding sequences. Automated sequencing was performed using vector- and gene-specific oligonucleotide primers. The sequence determined was submitted to GeneBank (BankIt486589 AF537188).

cDNA coding for human ataxin-3 was constructed by assembling the C-terminal coding sequence contained in IMAGE clone 79914 and the N-terminal coding sequence found in IMAGE clone number 4393766 (both purchased from the RZPD Deutsches Resourcenzentrum für Genomforschung GmbH). The assembled sequence was then subcloned into plasmid pGEX6P-1. Clones coding for Q26 and Q36 proteins were obtained by growing *Escherichia coli* cells, XL-1 blue strain, carrying the assembled gene inserted in pGEX6P-1 on LB-Ampicillin medium plates. Colonies were screened by PCR using gene-specific oligonucleotide primers. The number of glutamines was determined by automated sequencing using vector- and gene-specific oligonucleotide primers.

Protein Purification. The three ataxin-3 were expressed in *E. coli* strain BL21 codon plus RIL as GST-fusion proteins containing a PreScission Protease recognition site. Cells were grown at 37 °C in LB-ampicillin medium and induced with 50 μM IPTG at $A_{600} = 1.0$ for 2 h. About 13 g of cells was pelleted from 4 L of culture. To obtain crude extracts, cells were frozen and thawed, then incubated for 1 h at 4 °C in 100 mL of lysis buffer (10 mM sodium phosphate, pH 7.2, 150 mM NaCl, 1 mM phenylmethanesulfonyl fluoride, 10 mM DTT, 100 mM $MgCl_2$, 0.5 mg/mL lysozyme) and again frozen and thawed. 1% Triton-X-100 and DNase (0.2 mg/g of cells) were then added, and the samples were further incubated for 30 min at room temperature. Finally, they were centrifuged for 30 min at 47 000*g*. The supernatants were loaded onto a Glutathione Sepharose 4B affinity column (3 mL bed volume). The column was washed with three volumes of 10 mM sodium phosphate, pH 7.2, 150 mM NaCl, followed by three volumes of cleavage buffer (50 mM Tris-HCl, pH 7.0, 150 mM NaCl, 1 mM EDTA, 1 mM DTT). Removal of the GST affinity tail was achieved by incubating overnight at 4 °C the resin-bound proteins in the presence of PreScission Protease (400 U/mL resin). Mature ataxins-3 were then eluted with cleavage buffer, while PreScission Protease, being a GST fusion protein, remained bound to the resin. Ataxins were subsequently concentrated in Centricon YM-30 microconcentrators (Millipore Corporation, Bedford, MA) to final concentrations of 2−5 mg/mL.

SDS−PAGE and Western Blotting. SDS−PAGE was carried out according to Laemmli (*19*), in a Mighty Small apparatus (HoeferScientific Instruments, San Francisco, CA) with a 12% running gel and a 4% stacking gel. Proteins were revealed by Gel Code staining (Pierce Biotechnology, Rockford, IL). Western blot was performed according to Sambrook (*20*). Proteins were transblotted onto PVDF membranes and incubated in blocking solution (5% milk in PBS) for 60 min. Membranes were then probed for 60 min at 37 °C with either anti-human Q26 ataxin-3 polyclonal antibodies (Z46 antibodies) raised in rabbits using standard methods at 1:5000 in blocking solution or monoclonal antibody 1C2 purchased from Euromedex (Muindolsheim, France) at 1:2000 in blocking solution. After incubation in primary antibody, membranes were rinsed five times in 0.1% Tween in PBS for 5 min each and subsequently incubated for 30 min at 37 °C in secondary antibody (1:3000 horseradish peroxidase-goat anti-rabbit antibodies for Z46 primary antibody or 1:3000 horseradish-peroxidase-goat anti-mouse antibodies for IC2 primary antibody). Membranes were then rinsed as stated previously, and immunoreactive bands were

revealed using ECL Western blotting reagent (Amersham Biosciences UK Ltd., Little Chalfont, England).

Circular Dichroism. CD spectra were recorded on a Jasco J500A spectropolarimeter interfaced to a personal computer for data collection and manipulation and equipped with a thermostatically controlled cell holder. The data were analyzed by means of Jasco J700 software. The spectropolarimeter was calibrated with a d-10-camphorsulfonic acid solution. Protein samples were dissolved in 25 mM sodium phosphate, pH 7.0, 150 mM NaCl and analyzed in quartz cuvettes with 0.1 cm path length. Protein concentration (0.1 mg/mL) was determined on the basis of tyrosine and tryptophan absorbance at 280 nm. Spectra were recorded at different temperatures, after the signal was kept constant for at least 5 min. All protein spectra were baseline-corrected by subtracting buffer spectra. Molar mean residue ellipticity [θ] values were expressed for all wavelengths in deg cm^2 dmol^{-1} and were calculated by the equation [θ] = θMRW/10dc, were θ is the observed ellipticity in degrees, MRW the mean residue molecular mass of the examined protein, d is the optical path length in centimeters, and c is the protein concentration expressed in g/mL. Fractional composition in secondary structure for the three proteins was evaluated by the Convex Constraint Analysis method (*21*). When recording spectra at growing temperature, this was increased at a rate of about 1 °C/min. Before collection of each spectrum, samples were preincubated for 5 min. A total of 12 min was required to record an entire profile.

Congo Red Shift Assay. Amyloid fibril formation was detected as reported (*22*), with minor modifications. To elicit amyloidogenesis, human Q36 ataxin-3 (1 mg/mL) was heated at the same rate as in CD experiments. When the temperature attained 45, 55, and 75 °C, 60 μg samples were withdrawn, 10-fold diluted in 25 mM sodium phosphate, pH 7.0, 150 mM NaCl, 2.5 μM CR, and mixed thoroughly. After another 30 min incubation at room temperature, spectra were then recorded using a Jasco-550 spectrophotometer.

Electron Microscopy. Drops of the suspensions collected on collodion-carbon-coated grids were negatively stained with 4% sodium phosphotungstate, pH 4.0 and examined at a Zeiss 902 transmission electron microscope using 80 kV, 10 μA of beam current, 60 μm objective aperture, and an anticontamination device. Spectrometer facilities were routinelychecked to improve resolution and contrast. Magnification checks were routinely performed using a catalase standard. Specimen measurements were taken on negative films or on enlarged print using a lens with a micrometer.

RESULTS

Soluble Q6 Murine, Human Q26, and Q36 Ataxin-3 Are Obtained as Fusion Proteins with GST and in Mature Form After Proteolytic Removal of the Fusion Partner. The three mature ataxins-3 were subjected to SDS−PAGE to check their purity (Figure 1A), whereas their identity was confirmed by Western blotting, using either polyclonal antibodies against nonexpanded human ataxin-3 or 1C2 monoclonal antibodies, which are reported to preferentially recognize expanded, pathogenic polyQ stretches (*23*) (Figure 1B). As expected, murine ataxin-3 was not reactive toward 1C2. In contrast, the antibody recognized both human ataxins-3, Q26, and Q36, the latter being significantly more reactive than the former.

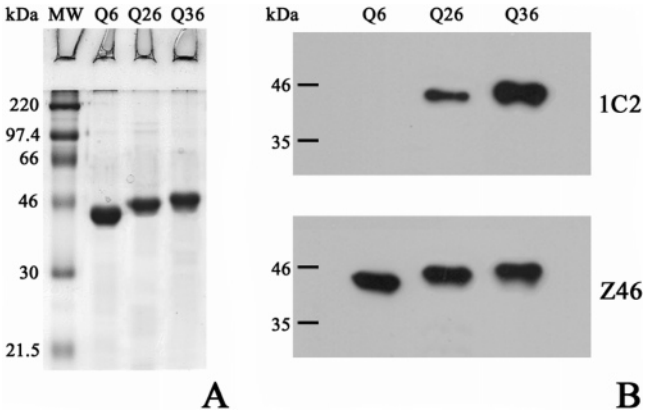

FIGURE 1: SDS−PAGE (12% gel) (A) and Western blot (B) of purified murine Q6, human Q26, and Q36 ataxins-3. Four micrograms of each protein was run in SDS−PAGE and revealed by Gel Code staining. Marker proteins with the respective molecular masses ($\times$ 10^{-3}) are also shown. For Western blot analysis, 100 ng of each protein was run and subsequently blotted onto PVDF. Proteins were immunodecorated either with 1C2 antibodies, or with Z46 antibodies, raised against human Q26 ataxin-3. The migration of marker proteins and their molecular masses are also indicated.

Ataxin-3 Is Endowed with a Remarkable Thermostability, Not Related to the Presence of polyQ. Far-UV CD spectra of murine (Q6) and human nonexpanded (Q26) and human moderately expanded (Q36) ataxins-3 were recorded at growing temperatures, up to 96 °C (Figure 2). At the lowest temperature, Q26 ataxin-3 displayed a relatively high helical content, in good agreement with the Q27 ataxin-3 spectrum previously reported (*17*). Spectra of the three proteins were similar but not identical to each other, the most evident difference being the weaker negative band at 222 nm in the murine form as compared to both human ataxins-3, which points to a lower helical content for the former protein. Furthermore, murine and human (Q26) ataxins-3 retained much of their secondary structure even at the highest temperature, the murine protein being slightly more temperature-sensitive than the human one (Figure 2, upper and middle panels). This highlights the unusual heat-resistance of the two proteins—at least as far as the secondary structure is concerned—and shows, at the same time, that it cannot be accounted for by the presence of the polyQ stretch. It should be also stressed, however, that in a previous work we observed a breakdown of the tertiary structure above 53 and 49 °C for murine and Q26 human proteins, respectively (*24*). This is reflected, to some extent, in their far-UV CD spectra (Figure 2), whose shapes undergo detectable changes starting from 50 °C, suggestive of a significant amount of non-native-like secondary structure above this temperature.

Human Q36 Ataxin-3 Undergoes a Temperature-Dependent, Conformational Transition, Followed by Irreversible Protein Precipitation. The CD spectrum of human, Q36 ataxin-3 underwent progressive changes starting from 40 °C. In particular, an assessment of secondary structure content (see Experimental Procedures) indicated an about 10% increase in β-structure and a comparable decrease in helical content when shifting the temperature from 37 to 80 °C (Figure 2, lower panel). However, above 80 °C, the protein underwent aggregation, which resulted in the formation of a visible precipitate. This prevented us from further collecting reliable spectra. We could not resolubilize the protein and

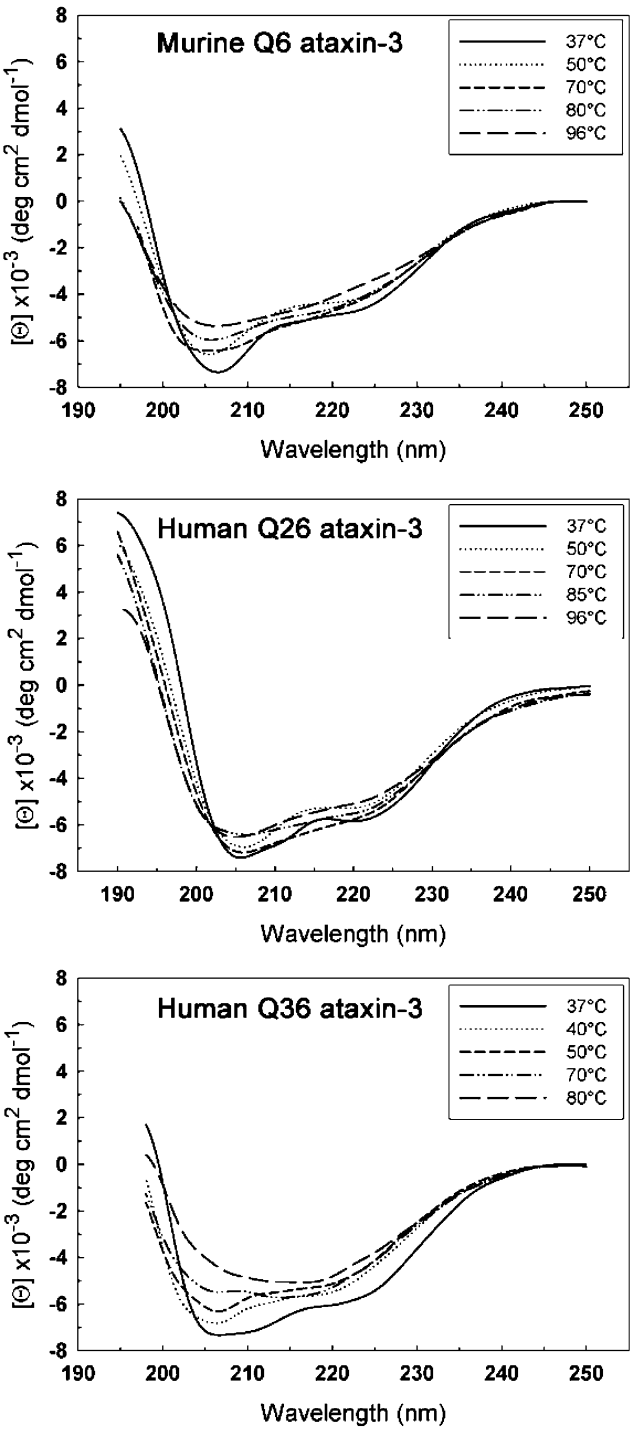

FIGURE 2: Far UV−CD spectra of ataxins-3 recorded at different temperatures of murine Q6, human Q26, and human Q36 ataxins-3. Protein samples (0.1 mg/mL) were dissolved in 25 mM sodium phosphate, pH 7.0, 150 mM NaCl. Optical path length was 0.1 cm.

reverse the conformational transition, even though the preparation was slowly cooled (data not shown). In contrast, human Q26 and murine ataxins-3 did not undergo any visible precipitation, even after an overnight incubation at 80 °C.

We also subjected to SDS−PAGE the precipitated Q36 ataxin-3. Staining did not evidence any band in the running gel. This was instead detected in the stacking gel (data not shown), suggestive of the appearance of SDS-resistant aggregates.

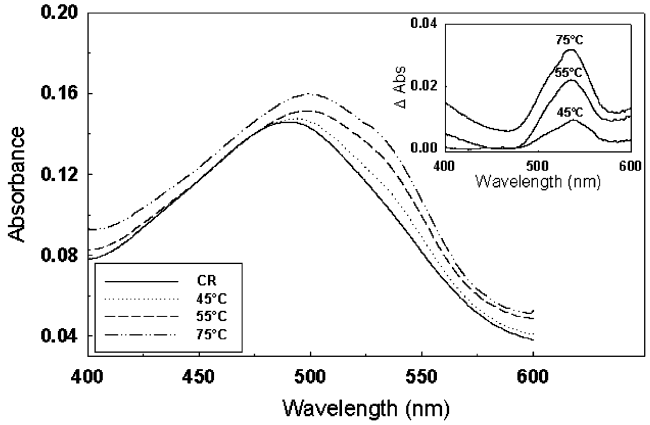

FIGURE 3: Congo red shift assay. Samples of human Q36 ataxin-3 preheated at the indicated temperatures were mixed with the dye (2.5 μM final concentration) in 25 mM sodium phosphate, pH 7.0, 150 mM NaCl. Spectra were recorded after another 30-min incubation at room temperature. A spectrum of the dye in the absence of the protein is also shown (solid line, CR). In the inset, difference spectra are shown: CR/protein−(CR alone + protein alone). For other details, see Experimental Procedures.

When Heated, Human Q36 Ataxin-3 Progressively Shifts Congo Red Spectrum. It is well-known that CR is able to specifically interact with amyloid fibrils, which results in a characteristic red shift and intensity increase of its visible spectrum (*22*). Thus, we probed human Q36 ataxin-3 for its ability to produce such spectral changes. After a 30 min preincubation at 45, 55, and 75 °C, the protein was mixed with the dye and incubated another 30 min at room temperature (Figure 3). Spectra recorded at 55 and 75 °C displayed the expected spectral shift, which was more pronounced at 75 °C. In contrast, the protein did not cause any spectral shift of CR after a 2 h preincubation at room temperature (data not shown).

Precipitated Human Q36 Ataxin-3 Molecules Pack Together to Yield Filaments of Different Sizes. Electron micrographs of negatively stained precipitates of Q36 ataxin-3 showed protofilaments of different lengths and a 2 ± 1.2 nm diameter (Figure 4A). They were apparently formed by individual globular entities, or protofibrils, with a slightly elongated shape and major and minor axes of approximately 2.7 and 2 nm, respectively. Protofilaments also showed the ability to pack together, mostly in an almost parallel fashion (Figure 4B) and to give rise to mature fibrils and bundles of larger size, not permeated by the negative stain (Figure 4C). Only occasionally amorphous aggregates were found, which shows that the aggregation did not result from protein thermal denaturation but is rather related to the amyloidogenic properties of the polyQ expansion.

Congo Red Retards the Heat-Induced Precipitation of Human Q36 Ataxin-3. Along with its well-known ability to specifically interact with amyloid fibrils—which results in a characteristic spectral shift (Figure 3 and ref *22*)—CR is also capable to prevent or retard their formation, so it is regarded as the prototypical antiamyloid agent (*12*, *22*). Thus, we probed its capacity to delay the heat-induced precipitation of Q36 ataxin-3. To do so, we incubated the protein at 85 °C in the presence of two different concentrations of the dye (i.e., 36 and 100 μM). It should be stressed that this experimental design is substantially different from that depicted in Figure 3, when the protein was preincubated at

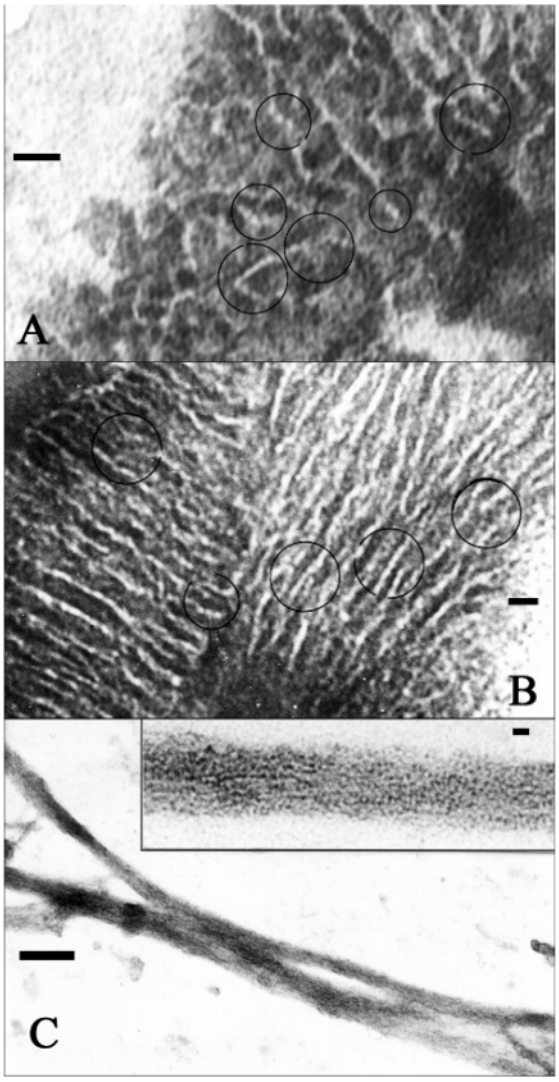

FIGURE 4: Electron micrographs of negatively stained Q36 ataxin 3 fibrils. Images were obtained using the spectrometer with ΔE = 0−10 eV. In the encircled zones, the globular substructure of the filaments is more evident. (A) Network of filaments. 680 000*x* (bar = 10 nm). (B) Parallel arrangement of single or associated filaments. 370 000*x* (bar = 10 nm). (C) Isolated large fibers. 75 000*x* (bar = 100 nm). The inset shows the detail of fiber surface composed of tightly packed globular filaments. 264 000*x* (bar = 10 nm).

different temperatures prior to addition of this compound. We thus observed a pronounced retardation of protein precipitation effected by CR and an almost complete prevention at the highest dye concentration (Figure 5A,B). Also, the effect was unquestionably specific, as different compounds structurally related to CR were either completely ineffective, or as in the case of tropaeolin, considerably less effective (Figure 6).

DISCUSSION

This work was undertaken to provide further insights into the mechanisms by which polyQ repeats affect the structure and behavior of polyglutaminated proteins. To this end, we characterized some variants of ataxin-3. Besides investigating human nonexpanded (Q26) and murine (Q6) ataxins-3, we focused in particular on a human form, whose polyQ tract is 36 residues long. This is the longest normal repeat reported so far for this protein. Unlike an expanded variant (Q78)

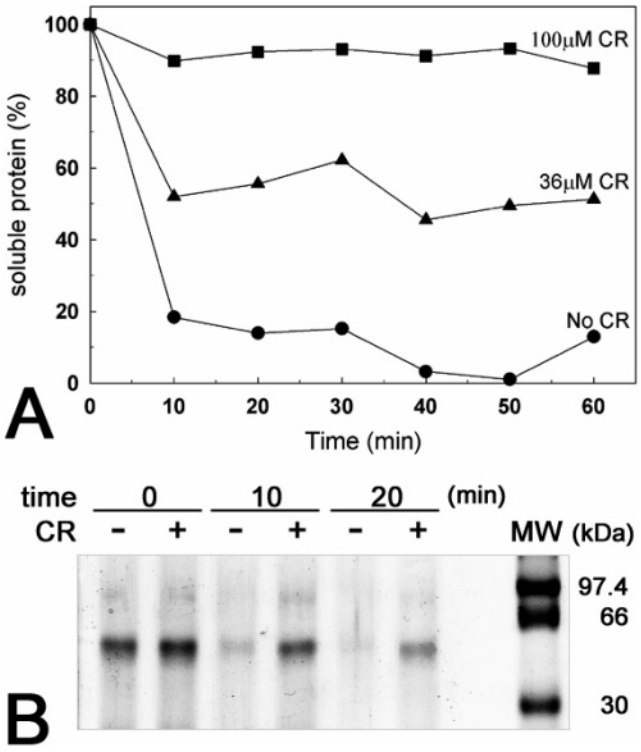

FIGURE 5: Time-dependent precipitation of Q36 ataxin-3 at 85 °C in the absence and the presence of CR. The protein (0.6 mg/mL) was incubated in 50 mM Tris-HCl, pH 7.0, 150 mM NaCl, 1 mM EDTA, 1 mM DTT. At the indicated times, samples were withdrawn and centrifuged at 16 000*g* for 10 min. The supernatants were either subjected to determinations of the residual soluble protein content (A) or to SDS−PAGE and Gel Code staining (B). In panel B, the CR concentration is 36 μM.

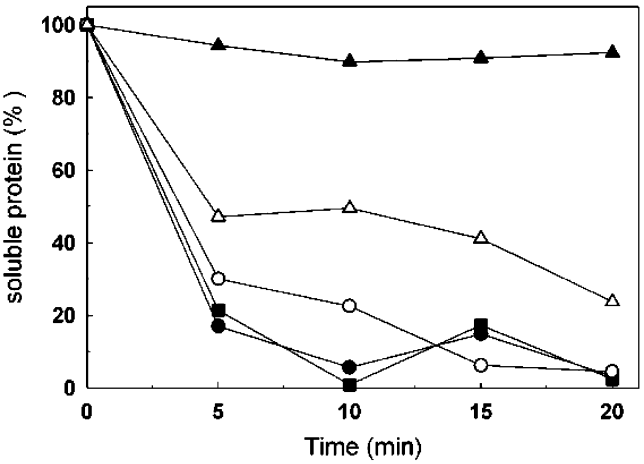

FIGURE 6: Effect of compounds structurally related to CR at a 100 μM concentration on the time-dependent precipitation of Q36 ataxin-3 at 85 °C. (▲) CR; (△) tropaeolin; (○) Orange G; (■) azobenzene; and (●) no addition. Proteins (0.6 mg/mL) were incubated in 50 mM Tris-HCl, pH 7.0, 150 mM NaCl, 1 mM EDTA, 1 mM DTT. At the indicated times, samples were withdrawn and centrifuged at 16 000*g* for 10 min, and the supernatants were subjected to determinations of the residual soluble protein content.

(*17*), all three forms here described were proven to be fully soluble at the physiological temperature.

As regards the murine protein, this is almost identical to the human form in the 291-residue long stretch upstream from the polyQ repeat, whereas it significantly diverges in the much shorter stretch downstream. Since several prediction

methods assign to this latter tract a disordered structure in both proteins, the ataxins-3 from either source plausibly possess a similar overall fold, except for the perturbing effects possibly brought about by the polyQ repeats. Thus, comparative investigations on these proteins should provide hints as to how the length of the repeats affects their structure and behavior.

Far-UV CD spectra did not evidence major differences among the three forms at room temperature. Furthermore, both murine and human Q26 ataxins-3 underwent marginal and reversible spectral changes up to about 90 °C, which highlights their remarkable heat resistance, at least as far as the secondary structure is concerned. On the other hand, in a previous work, we observed that the tertiary structure of the two proteins collapsed above 53 and 49 °C, respectively, as shown by several criteria (i.e., fourth derivative amplitude) near-UV CD and shift of the center of spectral mass (*24*). This points to a molten-globule-like structure for these proteins at temperatures higher than 50−55 °C. Whatever may be the reason of the heat resistance of the secondary structure, it cannot be related to the occurrence of the polyQ stretch, as the murine Q6 protein was almost as thermostable as the human Q26 form.

The major finding of the present work is, however, the heat-induced structural change of the human Q36 ataxin-3 and the subsequent protein precipitation. Actually, several lines of evidence indicate that the precipitates consist of amyloids, i.e., (a) the increase in β-structure (about 10%) and the concomitant decrease in helical content, shown by far-UV CD spectroscopy, in keeping with previous reports (*16*, *17*, *25*); (b) the ultramicroscopic observations; (c) the typical spectral shift of Cong red when added to the protein at growing temperatures; and (d) the ability of the dye to selectively prevent the heat-induced precipitation of this protein, when added prior to heating.

Thus, our results clearly show that the precipitates resulting from protein heating do represent authentic amyloid fibrils, although we cannot rule out, in principle, that the collapse of the tertiary structure, which takes place above 50−55 °C, may also favor amyloid formation.

These findings also raise the issue of what structure both normal and pathological expansions do possess. Structural modeling carried out recently (*26*) led to the proposal that nonexpanded polyQ tracts have a helical structure. However, in our opinion, the most plausible hypothesis is that they are disordered. Actually, this condition might allow non-expanded variants of polyglutaminated proteins to accommodate expansions differing in length of over 20 residues (*27*) without undergoing major structural changes, as suggested by their lack of any pathogenicity, either related to loss or to gain of function. This idea is also supported by CD analysis of artificial peptides (*14*), as well as by NMR studies on a fusion protein GST-Q22 (*15*).

Concerning expanded stretches, a recent model maintains that they consist of cylindrical β-sheets helically wound around the fiber axis and enclosing a central cylindrical cavity (*16*). According to the model, these structures have exactly 20 residues per turn, and two turns (i.e., 40 residues) is the minimum required to give rise a nucleation center for the formation of helical fibers. Residues in neighboring turns would be stabilized by hydrogen bonds between both their main chain and their side chain amides (*16*). Furthermore, the formation of the cylindrical sheet from a random coil state would be entropically favored despite the loss in conformational entropy. This is because the formation of intramolecular hydrogen bonds among the amides, which is associated to the transition, would result in release of bound water molecules (*16*). No suggestion is made in the aforementioned paper as regards the role of the enthalpic contribution. If, however, one assumes that the latter is negligible, an increase in temperature might substantially shift the equilibrium toward fiber formation by amplifying the entropic contribution. An additional, but not necessarily alternative, interpretation of the observed effect of the temperature is that it might favor the transition kinetically.

According to the model previously depicted, the 36-residue long polyQ stretch in our variant of ataxin-3 might be too short to give rise to amyloid fibrils. It should be stressed, however, that this protein has three more glutamines immediately upstream from the longer polyQ tract and a lysine between, which on the whole yields a 40-residue long expansion. Thus, it is conceivable that the lysine residue would accommodate in the two-turns-β-sheet resulting from the transition.

It should be also stressed that Q36 ataxin-3 is very close to the solubility threshold, as substantiated by the fact that we could not purify in significant amounts two other forms of human ataxin-3 carrying 40 and 52 consecutive glutamines, respectively. Actually, they were mostly found in pellets from *E. coli* cell extracts (data not shown), suggestive of extremely low solubility and/or propensity to tightly interact with other molecular partners. In particular, the former variant was obtained by replacing Lys^{295} by glutamine, which changed the polyQ sequence from Q_3KQ_{36} to Q_{40}. Thus, the replacement of just one amino acid was sufficient to dramatically drop protein solubility**.** The Q36 ataxin-3 variant, unlike those carrying longer polyQ stretches, represents therefore a suitable model for in vitro investigations on amyloid fiber formation. Furthermore, two advantages are associated with its handling: first, the process can be controlled by just increasing the temperature and second, this molecule is an authentic polyglutaminated protein and not an artificial construct, which involves that its behavior should be more representative of processes occurring in vivo.

On the whole, our observations and previous ones also suggest that the transition temperature should be inversely related to the length of the expansion, in keeping with the aforementioned insolubility at room temperature of human Q78 ataxin-3 (*17*) and the full solubility of Q26 at any temperature.

Another issue raised by the present paper is the interpretation of the electron micrographs of Q36 ataxin-3 preheated preparations. We observed filaments, apparently formed by individual, elongated globular entities, suggestive of a nucleation process by which the subunits assemble linearly to yield protofilaments. These can further pack together in a roughly parallel fashion and also may give rise to mature fibrils and bundles of larger size. These observations do not allow us to understand how β-sheets accommodate in the overall structure of the protein, nor how they would be able to interact with each other to produce linear assemblies of Q36 ataxin-3 molecules. Interestingly, very similar images have been reported for the amyloid-β40 protein (*28*). Whatever may be the interpretation of our results, they clearly

show, nevertheless, that no amorphous aggregate arose on heating the protein preparation.

Finally, our findings also pave the way to a fast and simple screening assay aimed at selecting antiamyloidogenic compounds. In fact, they should prevent or decrease the aggregation and the resulting clouding of Q36 ataxin-3 solutions on heat treatment, a process that can be easily monitored photometrically.

ACKNOWLEDGMENT

The skillful technical assistance of Marco Valtorta is gratefully acknowledged.

REFERENCES

1. Paulson, H. L. (1999) *Am. J. Hum. Genet. 64*, 339−345.
2. Zoghbi, H. Y., and Orr, H. T. (2000) *Annu. Rev. Neurosci. 23*, 217−247.
3. Gusella, J. F., and MacDonald, M. E. (2000) *Nat. Rev. Neurosci. 1*, 109−115.
4. Mandel, J. L. (1997) *Nature 386*, 767−769.
5. Perutz, M. F. (1996) *Curr. Opin. Struct. Biol. 6*, 848−858.
6. Perutz, M. F. (1999) *Trends Biochem. Sci. 24*, 58−63.
7. Perez, M. K., Paulson, H. L., and Pittman, R. N. (1999) *Hum. Mol. Genet. 8*, 2377−2385.
8. Ross, C. A., Poirier, M. A., Wanker, E. E., and Amzel, M. (2003) *Proc. Natl. Acad. Sci. U.S.A. 100*, 1−3.
9. Clarke, G., Collins, R. A., Leavitt, B. R., Andrews, D. F., Hayden, M. R., Lumsden, C. J., and McInnes, R. R. (2000) *Nature 406*, 195−199.
10. Perutz, M. F., and Windle, A. H. (2001) *Nature 412*, 143−144.
11. Bucciantini, M., Giannoni, E., Chiti, F., Baroni, F., Formigli, L., Zurdo, J., Taddei, N., Ramponi, G., Dobson, C. M., and Stefani, M. (2002) *Nature 416*, 507−511.
12. Sanchez, I., Mahlke, C., and Yuan, J. (2003) *Nature 421*, 373−379.
13. Heiser, V., Engemann, S., Brocker, W., Dunkel, I., Boeddrich, A., Waelter, S., Nordhoff, E., Lurz, R., Schugardt, N., Rautenberg, S., Herhaus, C., Barnickel, G., Bottcher, H., Lehrach, H., and Wanker, E. E. (2002) *Proc. Natl. Acad. Sci. U.S.A. 99* Suppl. 4, 16400−16406.
14. Altschuler, E. L., Hud, N. V., Mazrimas, J. A., and Rupp, B. (1997) *J. Pept. Res. 50*, 73−75.
15. Masino, L., Kelly, G., Leonard, K., Trottier, Y., and Pastore, A. (2002) *FEBS Lett. 513*, 267−272.
16. Perutz, M. F., Finch, J. T., Berriman, J., and Lesk, A. (2002) *Proc. Natl. Acad. Sci. U.S.A. 99*, 5591−5595.
17. Bevivino, A. E., and Loll, P. J. (2001) *Proc. Natl. Acad. Sci. U.S.A. 98*, 11955−11960.
18. Li, F., Macfarlan, T., Pittman, R. N., and Chakravarti, D. (2002) *J. Biol. Chem. 277*, 45004−45012.
19. Laemmli, U. K. (1970) *Nature 227*, 680−685.
20. Sambrook, J., Fritsch, E. F., and Maniatis, T. (1989) *Molecular Cloning: a Laboratory Manual*, 2nd ed., Cold Spring Harbor Laboratory, Cold Spring Harbor, NY.
21. Perczel, A., Park, K., and Fasman, G. D. (1992*) Anal. Biochem. 203*, 83−93.
22. Klunk, W. E., Jacob, R. F., and Mason, R. P. (1999) *Methods Enzymol. 309*, 285−305.
23. Trottier, Y., Lutz, Y., Stevanin, G., Imbert, G., Devys, D., Cancel, G., Saudou, F., Weber, C., David, G., Tora, L. et al. (1995) *Nature 378*, 403−406.
24. Marchal, S., Shehi, E., Harricane, M.-C., Fusi, P., Heitz, F., Tortora, P. and Lange, R. (2003) *J. Biol. Chem. 278*, 31554−31563.
25. Perutz, M. F., Pope, B. J., Owen, D., Wanker, E. E., and Scherzinger, E. (2002) *Proc. Natl. Acad. Sci. U.S.A. 99*, 5596−5600.
26. Albrecht, M., Hoffmann, D., Evert, B. O., Schmitt, I., Wullner, U., and Lengauer, T. (2003) *Proteins 50*, 355−370.
27. Durr, A., Stevanin, G., Cancel, G., Duyckaerts, C., Abbas, N., Didierjean, O., Chneiweiss, H., Benomar, A., Lyon-Caen, O., Julien, J., Serdaru, M., Penet, C., Agid, Y., and Brice, A. (1996) *Ann. Neurol. 39*, 490−499.
28. Harper, J. D., Wong, S. S., Lieber, C. M., and Lansbury, P. T., Jr. (1999) *Biochemistry 38*, 8972−8980.

BI0352825